Standardizing Human Brain Parcellations

Patrick E. Myers[1], Ganesh C. Arvapalli[1], Sandhya C.Ramachandran[1], Derek A. Pisner[2], Paige F. Frank[1], Allison D. Lemmer[1], Eric W. Bridgeford[1], Aki Nikolaidis[3], Joshua T. Vogelstein[1], *

Abstract. Using brain atlases to localize regions of interest is a required for making neuroscientifically valid statistical inferences. These atlases, represented in volumetric or surface coordinate spaces, can describe brain topology from a variety of perspectives. Although many human brain atlases have circulated the field over the past fifty years, limited effort has been devoted to their standardization and specification. The purpose of standardization and specification is to ensure consistency and transparency with respect to orientation, resolution, labeling scheme, file storage format, and coordinate space designation. Consequently, researchers are often confronted with limited knowledge about a given atlas's organization, which make analytic comparisons more difficult. To fill this gap, we consolidate an extensive selection of popular human brain atlases into a single, curated open-source library, where they are stored following a standardized protocol with accompanying metadata. We propose that this protocol serves as the basis for storing future atlases. To demonstrate the utility of storing and standardizing these atlases following a common protocol, we conduct an experiment using data from the Healthy Brain Network whereby we quantify the statistical dependence of each atlas label on several key phenotypic variables. The repository containing the atlases, the specification, as well as relevant transformation functions is available at https://neurodata.io/mri

Background & Summary Understanding the brain's organization is one of the key challenges in human neuroscience [1] and is critical for clinical translation [2]. Parcellation of the brain into functionally and structurally distinct regions has seen impressive advances in recent years [3], and has grown the field of network neuroscience [4, 5]. Through a range of techniques such as clustering [6–9], multivariate decomposition [10, 11] , gradient based connectivity [1, 12–16], and multimodal neuroimaging [1], parcellations have enabled fundamental insights into the brain's topological organization and network properties [17]. In turn, these properties have allowed researchers to investigate brain-behavioral associations with developmental [18, 19], cognitive [20, 21], and clinical phenotypes [22–24].

More recently, researchers interested in understanding brain organization are presented with a variety of brain atlases that can be used to define nodes of network-based analyses [25]. While this variety is a boon to researchers, the use of different parcellations across studies makes assessing reproducibility of brain-behavior relationships difficult (e.g. comparing across parcellations with different organizations and numbers of nodes; [5]). Amalgamating multiple brain parcellations into a single, standardized, curated list would offer researchers a valuable resource for evaluating replication of neuroimaging studies.

Some efforts to consolidate these atlases is already underway. For example, Nilearn is a popular Python package that provides machine-learning and informatics tools for neuroimaging [26]. Nilearn provides several single line command line interface functions to 'fetch' both atlases and datasets. Nilearn includes twelve anatomically and functionally defined atlases, such as the Harvard-Oxford [27] and Automated Anatomical Labeling (AAL) [28] parcellation. Although a promising prototype, Nilearn's current atlas collection represent a limited range of available atlases, and the more recent gradient based, surface based, and multimodal parcellations have yet to be included into any central repository. More importantly, existing atlas repositories have not attempted to systematically standardize their collections following a single specification. Without well-established standards, the investigator is faced with limited information about each atlas, so connecting neuroscientific findings to the organization of the atlas becomes more difficult. Moreover, if the investigator requires a comparison across atlases, some form of metadata must be available that describes the similarities and differences between them.

Neuroparc mitigates these issues by providing: (1) a detailed atlas specification which will enable researchers to both easily understand existing atlases and generate new atlases compliant with this specification, (2) a repository of the most commonly used atlases in neuroimaging, all stored in that

---

*Corresponding author: Joshua T. Vogelstein jovo@jhu.edu; [1] Johns Hopkins University, [2] University of Texas at Austin, [3] Child Mind Institute.

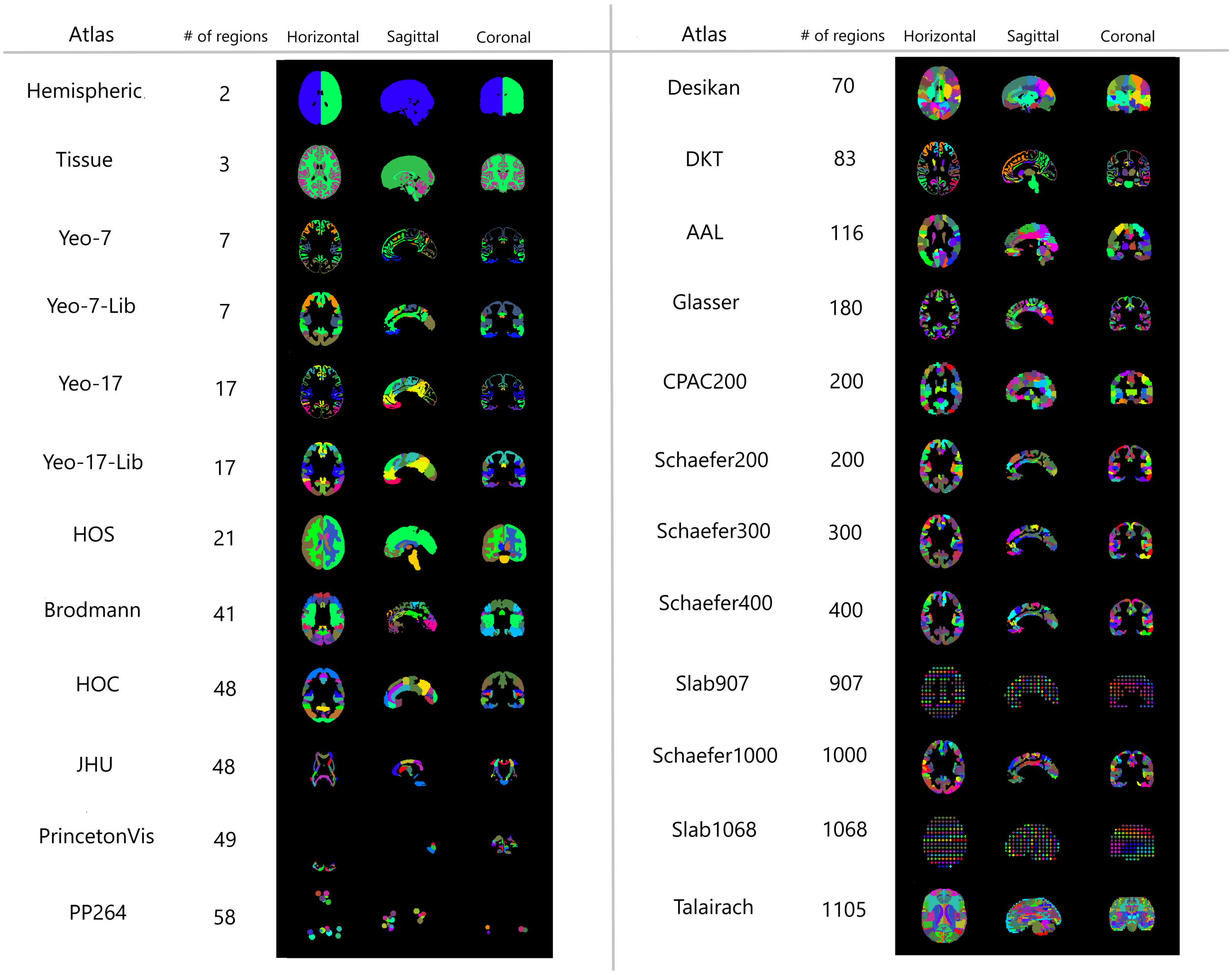

Atlas	# of regions	Horizontal	Sagittal	Coronal
Hemispheric	2			
Tissue	3			
Yeo-7	7			
Yeo-7-Lib	7			
Yeo-17	17			
Yeo-17-Lib	17			
HOS	21			
Brodmann	41			
HOC	48			
JHU	48			
PrincetonVis	49			
PP264	58			
Desikan	70			
DKT	83			
AAL	116			
Glasser	180			
CPAC200	200			
Schaefer200	200			
Schaefer300	300			
Schaefer400	400			
Slab907	907			
Schaefer1000	1000			
Slab1068	1068			
Talairach	1105			

Figure 1: A comparison of the regions present in the major atlases available in Neuroparc. These visualizations were made using MIPAV tri-planar views on the same slice numbers. Each atlas shows a cross-section in each of the canonical orthogonal planes (H=Horizontal, S=Sagittal, C=Coronal). For most atlases, the slice numbers were (90, 108, 90). There are a few exceptions for visualization purposes: JHU: (90, 108, 109), Slab907: (95, 104, 95), Slab1068: (93, 105, 93) [30–40]

specification, and (3) a set of functions for transforming, comparing, and visualizing these atlases. The Neuroparc package presented here includes 24 different adult human brain parcellations—including surface-based and volume-based. Here, we provide an overview of the relationship between these parcellations via comparison of the spatial similarity between atlases, as measured by Dice coefficient. To validate the atlases and their utility, we provide an prototypical analysis of brain-behavior relationships in these parcellations across a range of phenotypic variables from a large publicly available developmental sample: the Healthy Brain Network [29]. To facilitate replication and extension of this work, all the data and code are available from https://neurodata.io/mri.

Methods

Data Compilation Neuroparc contains atlases from several locations. As previously noted, there is no current standard for atlas storage, so all gathered datasets are converted into a single format. We define this human brain atlas specification in detail within Data Records.

Dice Coefficient The Dice coefficient is a measure of similarity between two sets [41]. Specifically, it measures a coincidence index (CI) between two sets, normalized by the size of the sets. Let h be the number of points overlapping in the sets A and B, and a and b are the sizes of their corresponding sets. If the two sets are labelled regions in segmented images, then the Dice coefficient between any pair of regions between the images is given by

$$CI_{ij} = \frac{2h_{ij}}{a_i + b_j} \tag{0.1}$$

where i is the region in image 1 and j is the region in image 2. The result is a similarity matrix, as shown in Figure 2. Since this map visualizes similarity between two regions in two atlases, the information provided by the Dice map can be used quantify which regions in a given atlas are most similar to regions in another atlas.

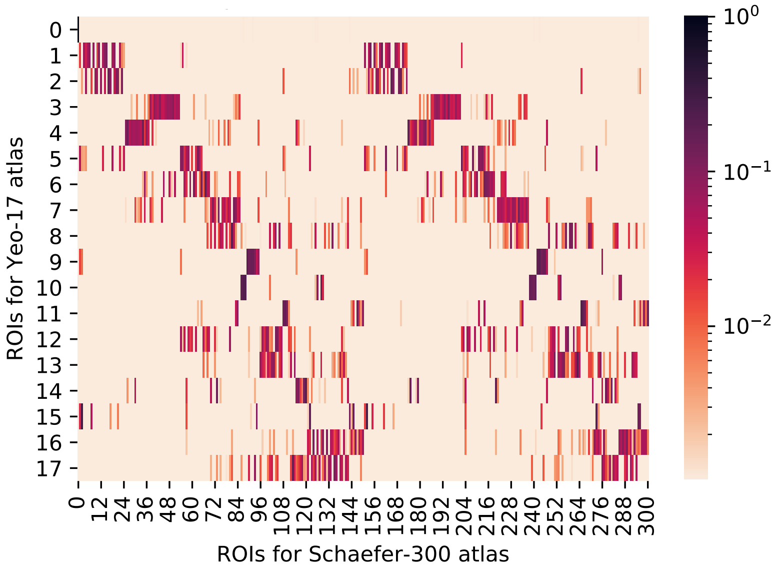

Figure 2: Dice Score Map between the Yeo 17 Networks atlas and the 300 parcellation Schaefer atlas. The strong symmetry of the Yeo atlas is apparent here.

Adjusted Mutual Information Adjusted mutual information is another measure of the similarity of two labelled sets, quantifying how well a particular point can be identified as belonging to a region given another region. It differs from the Dice coefficient in that it tends to be more sensitive to region size and position relative to other measures. [42]

Similar to the Dice coefficient, Adjusted mutual information is not dependent on a region's label [43]. Volumes that share many points are likely to be have a higher mutual information score all else being equal [44].

To assure that all atlas comparisons were on the same scale, Neuroparc computes the adjusted mutual information score. Let $H(\cdot)$ denote entropy, N be the number of elements (voxels) in total, and $E(MI_AB)$ denote the expected mutual information for sets of size a and b. Here, $P_A(i)$ is the probability that a point chosen randomly from the set A will belong to region i. [45]

$$H(A) = -\sum_{i=1}^{N} P_A(i) log(P_A(i)) \tag{0.2}$$

$$MI_{AB} = \sum_{a,b} P_{A,B}(a,b) \cdot \log \frac{P_{A,B}(a,b)}{P_A(a) \cdot P_B(b)} \tag{0.3}$$

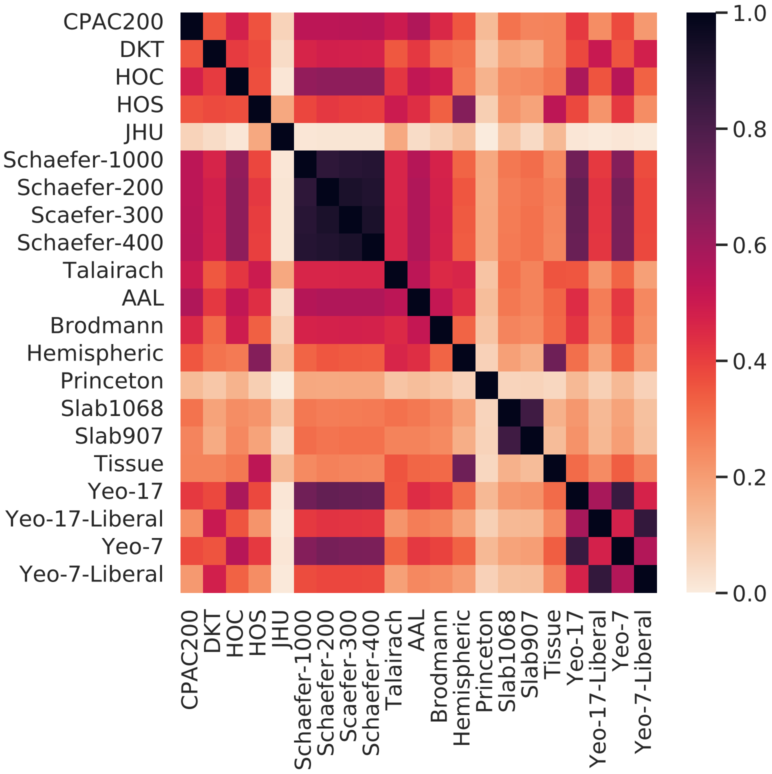

Figure 3: The adjusted mutual information between atlases contained within Neuroparc. The Schaefer atlases contain a high degree of mutual information as expected as they were built using the same algorithm.

where $P_{A,B}(a,b)$ is the probability that a voxel will belong to region a in set A and region b in set B.
(0.4)

$$E[MI(A,B)] = \sum_{i=1}^{N}\sum_{j=1}^{N}\sum_{n_{ij}=(a_i+b_j-N)^+}^{min(a_i,b_j)} \frac{n_{ij}}{N}\log\left(\frac{N\cdot n_{ij}}{a_i b_j}\right)\frac{a_i!b_j!(N-a_i)!(N-b_j)!}{N!n_{ij}!(a_i-n_{ij})!(N-a_i-b_j+n_{ij})!}$$

where a_i is the number of voxels in region i of set A and b_j is the number of voxels in region j of set B. $(a_i+b_j-N)^+ = max(1, a_i+b_j-N)$.

$$AMI_{AB} = \frac{MI_{AB} - E(MI_{AB})}{mean(H(A),H(B)) - E(MI_{AB})} \tag{0.5}$$

as provided in [46].

Figure 3 shows the adjusted mutual information between all pairs of atlases. The information provided for this score is atlas-wide, while the Dice score was computed per region to generate a map. The similarity between groups of atlases, such as the various Schaefer atlases, and the Yeo liberal atlases, is immediately apparent.

Code availability Code for processing is publicly available and can be found on GitHub under the scripts folder (https://github.com/neurodata/neuroparc). Examples of useful functions include center calculation for regions and scripts to save files in the NIfTI format. All code is provided under the Apache 2.0 License.

Visualizations are generated using both MIPAV 8.0.2 and FSLeyes 5.0.10 to view the brain volumes in 2D and 3D spaces [47, 48]. Figure 1 can be created using MIPAV triplanar views of each atlases with a striped LUT.

Data Records All data records described in this paper are available primarily through a Github repository; a link is available from https://neurodata.io/mri. Several file types are contained in this location and are necessary for fully describing an atlas. Neuroparc introduces an atlas specification that includes a reference brain, an atlas file, and atlas metadata.

Reference Brain To allow direct comparison between different atlases, a standard reference brain must be used for all involved atlases. Within Neuroparc, a single reference brain is provided, yielding a coordinate space. Neuroparc uses Montreal Neurological Institute 152 Nonlinear 6th generation reference brain, abbreviated MNI152NLin6 in the file naming structure [49].

The brain is stored in a GNU-zipped NIfTI file format of a T1 weighted MRI.Three image resolutions are available in Neuroparc (1mm, 2mm, and 4mm) for flexibility. The naming convention for these files is: MNI152Nlin6_res-<*resolution*>_T1W.nii.gz. The format of the *resolution* input would be 1x1x1 for the 1 mm^3 resolution.

Atlas Image The atlas image is also a GNU-zipped NifTi file containing the parcellated reference brain according to the specifications of the atlas. The file indicates to which region each voxel belongs. Each region of interest (ROI) within this parcellated image is denoted by a unique integer ranging from 1 to n where n is the total number of ROIs. The naming convention for the atlas is: <*atlas_name*>_space-MNI152NLin6_res–<*resolution*>.nii.gz. The *atlas_name* field is unique for each atlas image, ideally no more than two words long without a space in between (e.g. yeo-17, princetonvisual, HarvardOxford).

For simplicity, only the 1 mm^3 resolution parcellation is stored within the repository, but other resolutions can be calculated from the reference brain images.

Atlas Metadata The metadata corresponding to the atlas is contained within a JSON file format. This file is split into two sections: region-wide and atlas-wide information.

The region-wide data must contain the number, label, center, and size for that region. The center and size can be calculated using provided code in Neuroparc.

Although label must be specified, this information is not relevant for all atlases. In that case, NULL should be used for the labels of the regions. For hierarchical regions, the naming should be in order of largest region to smallest with a '.' in between each name. An example of this is in the Talairach atlas, which contains the region with label "Right Cerebrum.Parietal Lobe.Sub-Gyral.Gray Matter.Brodmann area 40".

Optional fields in the region-wide data include description and color. Description can be used to provide more information than the region label if necessary. An example of this use is in the Yeo-7 Networks atlas. The label for this atlas is in the form '7Networks_2', but the description for that label is the corresponding functional network, 'Somatomotor' in this case. The color field must be given in the form [R, G, B] and is only used if the user wants to specify the colors of the regions upon visualization.

Brain-wide data must include the name, description, native coordinate space, and source of the atlas. The name field allows for more elaboration than in the name of the file. The description is more flexible, allowing the creator of an atlas to briefly describe important information for users of their atlas. The intended use case or the method of generation are examples of information provided in this field. Since all atlases in Neuroparc are stored in the same coordinate space, the coordinate space used during the creation of the atlas must be specified.

Finally, the publication detailing the atlas should be included in the source field so users can have a more full understanding of the atlas being used. Optional fields for brain-wide data can all be calculated, including the number of regions, the average volume per region, whether the segmented regions are hierarchical, and if the atlas is symmetrical.

The naming convention for this file is as follows:

<*atlas_name*>_space-MNI152NLin6_res-1x1x1.json

Again, this metadata is only relevant to the 1 mm^3 resolution, but other data is easily calculated when necessary.

The full description and format of the atlas specification is available within Neuroparc at https:

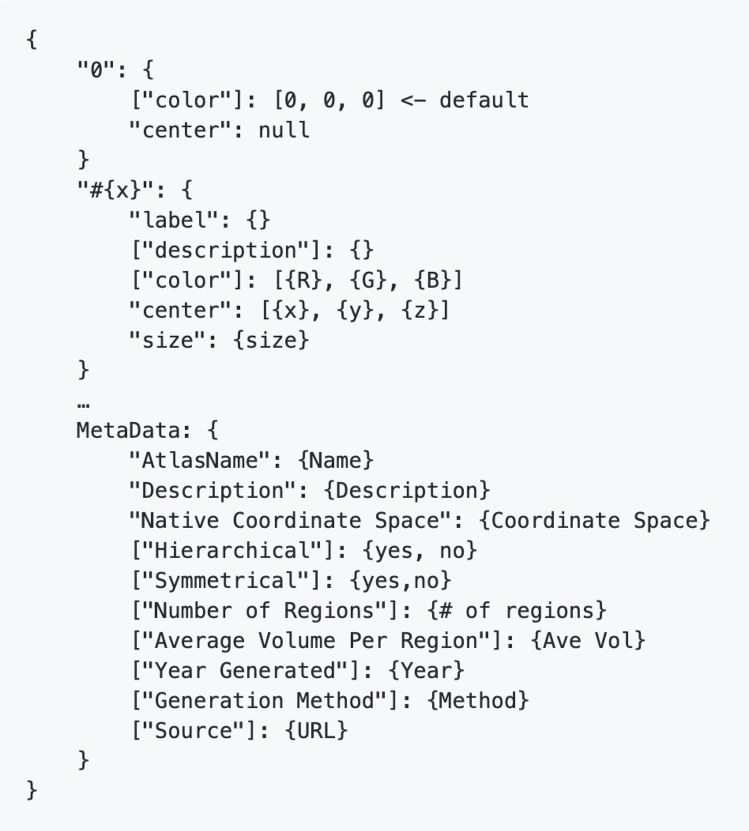

```
{
    "0": {
        ["color"]: [0, 0, 0] <- default
        "center": null
    }
    "#{x}": {
        "label": {}
        ["description"]: {}
        ["color"]: [{R}, {G}, {B}]
        "center": [{x}, {y}, {z}]
        "size": {size}
    }
    …
    MetaData: {
        "AtlasName": {Name}
        "Description": {Description}
        "Native Coordinate Space": {Coordinate Space}
        ["Hierarchical"]: {yes, no}
        ["Symmetrical"]: {yes,no}
        ["Number of Regions"]: {# of regions}
        ["Average Volume Per Region"]: {Ave Vol}
        ["Year Generated"]: {Year}
        ["Generation Method"]: {Method}
        ["Source"]: {URL}
    }
}
```

Figure 4: An example json file storing atlas metadata

//neurodata.io/mri. Figure 4 shows an example json file.

Technical Validation All atlases included in Neuroparc have been pulled from reputable published sources [30–40] and modified to fit the above described atlas specification. Specifically, all of the atlas images were converted into the Montreal Neurological Institute 152 Nonlinear 6th generation coordinate space. All of the atlases were applied to the single T1 weighted MRI scan so that each atlas is directly comparable.

To demonstrate the validity of these atlases, we conduct the following case study. The Healthy Brain Network (HBN) is a relatively new dataset that consists of over 1,000 children and adolescents in New York City. HBN was created to study mental health and learning disorders. HBN includes phenotypic data in the form of tests on psychiatric, behavioral, cognitive, and lifestyle, as well as multimodal brain imaging, electroencephalography, digital voice and video recordings, genetics, and actigraphy. In this analysis, 'MGC', an independence test implemented in the python package 'mgcpy' was used to test for correlation between functional connectomes and phenotypic data [50, 51]. We ran the NDMG pipeline on every individuals' resting state functional MRI data to obtain connectomes for each. [52]. We then selected 23 assays to test for a dependence between the connectomes on various phenotypic properties. Doing so required carefully cleaning and purging the subject level questionnaire answers to eliminate missing data and spurious entries. The number of individuals whose data were available per test are outlined in Table 1.

For each phenotypic test and each atlas, we ran MGC to test whether connectomes and cognitive assays were statistically dependent on one another (Figure 5). Assays generally had either multiple atlases which found a significant correlation ($\alpha \leq 0.05$), or none. The assays which had a significant correlation for some atlases were APQ_SR, ASSQ, CELF_5_Screen, MFQ_P, PAQ_C, and SWAN. APQ_P, MFQ_SR, and PAQ_A which are the same tests but for a different age group as APQ_SR,

Test	#Subjects	Category
ACE	16	Family Structure, Stress and Trauma
APQ_SR	288	Family Structure, Stress and Trauma
ARI_P	307	Depression and Mood
ARI_S	306	Depression and Mood
ASR	12	Multiple Disorders
ASSQ	313	Autism Spectrum Disorder
AUDIT	135	Substance Abuse/Addictive Behavior
Barratt	322	Background Information and Demographics
CELF_5_Screen	279	Verbal Learning
Digit_Span	126	Cognitive and Executive Functioning
IAT	93	Substance Abuse/Addictive Behavior
MFQ_P	118	Depression and Mood
MFQ_SR	125	Depression and Mood
PAQ_A	64	Physical
PAQ_C	155	Physical
PCIAT	136	Substance Abuse/Addictive Behavior
PSI_P	98	Family Structure, Stress and Trauma
SCARED_P	237	Anxiety
SCARED_SR	226	Anxiety
SDS	121	Sleep
STAI	15	Anxiety
SWAN	301	Attention-Deficit/Hyperactivity Disorder
YSR	93	Multiple Disorders

Table 1: This table shows the number of subjects analyzed for each assay as well as the category of the corresponding test.

MFQ_P, and PAQ_C. The APQ, ASSQ, CELF_5_Screen, MFQ, PAQ, and SWAN are in the categories Family Structure Stress and Trauma, ASD, Verbal Learning, Depression and Mood, Physical, and ADHD as given by the Child Mind Institute. There does not appear to be a strong connection from this alone between category of test and whether significant correlation is found. ACE, a questionnaire on the occurrence various traumatic childhood events, SCARED_P, an anxiety test for preschoolers, and PAQ_A, a questionnaire on physical activity all also showed extremely high p-values.

Interestingly, the same tests but given in the regular version or the preschooler version frequently had very different results. This appears to indicate that such tests might have more correlation with brain connectivity and structure within different age groups.

Medians over all atlases show the results discussed above. Medians over all tests are all fairly high and not very distinct. The tissue atlas has the highest average p-value, and the HarOxCort atlas has the lowest, ranging from about 0.35 to 0.55. This does not account for whether or not the atlas is correctly finding correlations and is an average over relatively few tests, so it is hard to interpret. It would be interesting to investigate this variation more, possibly when averaging over a higher number of tests than this analysis.

Usage Notes The Usage Notes should contain brief instructions to assist other researchers with reuse of the data. This may include discussion of software packages that are suitable for analysing the assay data files, suggested downstream processing steps (e.g. normalization, etc.), or tips for integrating or comparing the data records with other datasets. Authors are encouraged to provide code, programs or data-processing workflows if they may help others understand or use the data. Please see our code

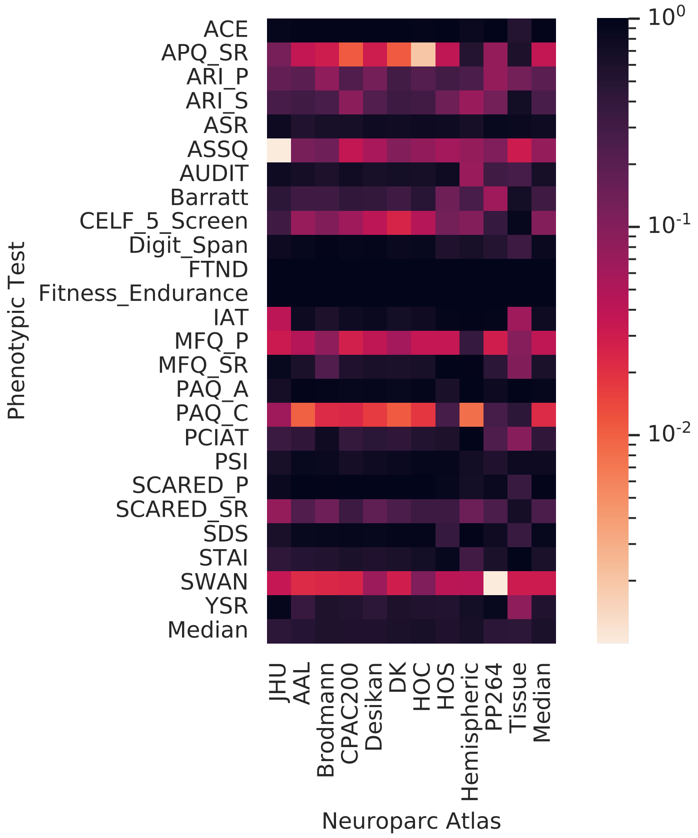

Figure 5: This plot shows the p-value calculated by 'mgc' between each phenotypic test and the functional connectomes for each atlas. It is in the form of a heatmap with range 0 to 1, using a log scale. On the far right and far bottom, the median values over the rows and columns are shown.

availability policy for advice on supplying custom code alongside Data Descriptor manuscripts.

For studies involving privacy or safety controls on public access to the data, this section should describe in detail these controls, including how authors can apply to access the data, what criteria will be used to determine who may access the data, and any limitations on data use.

Acknowledgements We would like to acknowledge generous support from National Science Foundation (NSF) under NSF Award Number EEC-1707298.

*corresponding author: jovo@jhu.edu

References

[1] Matthew F Glasser, Timothy S Coalson, Emma C Robinson, Carl D Hacker, John Harwell, Essa Yacoub, Kamil Ugurbil, Jesper Andersson, Christian F Beckmann, Mark Jenkinson, et al. A multi-modal parcellation of human cerebral cortex. *Nature*, 536(7615):171, 2016.

[2] Michael D Fox and Michael Greicius. Clinical applications of resting state functional connectivity. *Frontiers in systems neuroscience*, 4:19, 2010.

[3] Simon B Eickhoff, BT Thomas Yeo, and Sarah Genon. Imaging-based parcellations of the human brain. *Nature Reviews Neuroscience*, page 1, 2018.

[4] Patric Hagmann, Maciej Kurant, Xavier Gigandet, Patrick Thiran, Van J Wedeen, Reto Meuli, and Jean-Philippe Thiran. Mapping human whole-brain structural networks with diffusion mri. *PloS one*, 2(7):e597, 2007.

[5] Andrew Zalesky, Alex Fornito, Ian H Harding, Luca Cocchi, Murat Yücel, Christos Pantelis, and Edward T Bullmore. Whole-brain anatomical networks: does the choice of nodes matter? *Neu-*

roimage, 50(3):970–983, 2010.

[6] Pierre Bellec, Pedro Rosa-Neto, Oliver C Lyttelton, Habib Benali, and Alan C Evans. Multi-level bootstrap analysis of stable clusters in resting-state fmri. *Neuroimage*, 51(3):1126–1139, 2010.

[7] R Cameron Craddock, G Andrew James, Paul E Holtzheimer III, Xiaoping P Hu, and Helen S Mayberg. A whole brain fmri atlas generated via spatially constrained spectral clustering. *Human brain mapping*, 33(8):1914–1928, 2012.

[8] Aki Nikolaidis, Anibal Solon Heinsfeld, Ting Xu, Pierre Bellec, Joshua Vogelstein, and Michael Milham. Bagging improves reproducibility of functional parcellation. *bioRxiv*, page 343392, 2019.

[9] Bertrand Thirion, Gaël Varoquaux, Elvis Dohmatob, and Jean-Baptiste Poline. Which fmri clustering gives good brain parcellations? *Frontiers in neuroscience*, 8:167, 2014.

[10] Christian F Beckmann, Clare E Mackay, Nicola Filippini, and Stephen M Smith. Group comparison of resting-state fmri data using multi-subject ica and dual regression. *Neuroimage*, 47(Suppl 1): S148, 2009.

[11] Gaël Varoquaux, Alexandre Gramfort, Fabian Pedregosa, Vincent Michel, and Bertrand Thirion. Multi-subject dictionary learning to segment an atlas of brain spontaneous activity. In *Biennial International Conference on Information Processing in Medical Imaging*, pages 562–573. Springer, 2011.

[12] Alexander L Cohen, Damien A Fair, Nico UF Dosenbach, Francis M Miezin, Donna Dierker, David C Van Essen, Bradley L Schlaggar, and Steven E Petersen. Defining functional areas in individual human brains using resting functional connectivity mri. *Neuroimage*, 41(1):45–57, 2008.

[13] Evan M Gordon, Timothy O Laumann, Babatunde Adeyemo, Jeremy F Huckins, William M Kelley, and Steven E Petersen. Generation and evaluation of a cortical area parcellation from resting-state correlations. *Cerebral cortex*, 26(1):288–303, 2014.

[14] Steven M Nelson, Alexander L Cohen, Jonathan D Power, Gagan S Wig, Francis M Miezin, Mark E Wheeler, Katerina Velanova, David I Donaldson, Jeffrey S Phillips, Bradley L Schlaggar, et al. A parcellation scheme for human left lateral parietal cortex. *Neuron*, 67(1):156–170, 2010.

[15] Gagan S Wig, Timothy O Laumann, Alexander L Cohen, Jonathan D Power, Steven M Nelson, Matthew F Glasser, Francis M Miezin, Abraham Z Snyder, Bradley L Schlaggar, and Steven E Petersen. Parcellating an individual subject's cortical and subcortical brain structures using snowball sampling of resting-state correlations. *Cerebral cortex*, 24(8):2036–2054, 2013.

[16] Ting Xu, Alexander Opitz, R Cameron Craddock, Margaret J Wright, Xi-Nian Zuo, and Michael P Milham. Assessing variations in areal organization for the intrinsic brain: from fingerprints to reliability. *Cerebral Cortex*, 26(11):4192–4211, 2016.

[17] Daniel S Margulies, Satrajit S Ghosh, Alexandros Goulas, Marcel Falkiewicz, Julia M Huntenburg, Georg Langs, Gleb Bezgin, Simon B Eickhoff, F Xavier Castellanos, Michael Petrides, et al. Situating the default-mode network along a principal gradient of macroscale cortical organization. *Proceedings of the National Academy of Sciences*, 113(44):12574–12579, 2016.

[18] Nico UF Dosenbach, Binyam Nardos, Alexander L Cohen, Damien A Fair, Jonathan D Power, Jessica A Church, Steven M Nelson, Gagan S Wig, Alecia C Vogel, Christina N Lessov-Schlaggar, et al. Prediction of individual brain maturity using fmri. *Science*, 329(5997):1358–1361, 2010.

[19] Franziskus Liem, Gaël Varoquaux, Jana Kynast, Frauke Beyer, Shahrzad Kharabian Masouleh, Julia M Huntenburg, Leonie Lampe, Mehdi Rahim, Alexandre Abraham, R Cameron Craddock, et al. Predicting brain-age from multimodal imaging data captures cognitive impairment. *Neuroimage*, 148:179–188, 2017.

[20] Emily S Finn, Xilin Shen, Dustin Scheinost, Monica D Rosenberg, Jessica Huang, Marvin M Chun, Xenophon Papademetris, and R Todd Constable. Functional connectome fingerprinting: identifying individuals using patterns of brain connectivity. *Nature neuroscience*, 18(11):1664, 2015.

[21] Zarrar Shehzad, Clare Kelly, Philip T Reiss, R Cameron Craddock, John W Emerson, Katie McMahon, David A Copland, F Xavier Castellanos, and Michael P Milham. A multivariate distance-based analytic framework for connectome-wide association studies. *Neuroimage*, 93:74–94, 2014.

[22] Alexandre Abraham, Michael P Milham, Adriana Di Martino, R Cameron Craddock, Dimitris Samaras, Bertrand Thirion, and Gael Varoquaux. Deriving reproducible biomarkers from multi-site resting-state data: an autism-based example. *NeuroImage*, 147:736–745, 2017.

[23] Deanna J Greene, Jessica A Church, Nico UF Dosenbach, Ashley N Nielsen, Babatunde Adeyemo, Binyam Nardos, Steven E Petersen, Kevin J Black, and Bradley L Schlaggar. Multivariate pattern classification of pediatric tourette syndrome using functional connectivity mri. *Developmental science*, 19(4):581–598, 2016.

[24] Seok-Jun Hong, Sofie L Valk, Adriana Di Martino, Michael P Milham, and Boris C Bernhardt. Multidimensional neuroanatomical subtyping of autism spectrum disorder. *Cerebral Cortex*, 28 (10):3578–3588, 2017.

[25] Salim Arslan, Sofia Ira Ktena, Antonios Makropoulos, Emma C Robinson, Daniel Rueckert, and Sarah Parisot. Human brain mapping: A systematic comparison of parcellation methods for the human cerebral cortex. *Neuroimage*, 170:5–30, 2018.

[26] Alexandre Abraham, Fabian Pedregosa, Michael Eickenberg, Philippe Gervais, Andreas Mueller, Jean Kossaifi, Alexandre Gramfort, Bertrand Thirion, and Gael Varoquaux. Machine learning for neuroimaging with scikit-learn. *Frontiers in Neuroinformatics*, 8:14, 2014. ISSN 1662-5196. doi: 10.3389/fninf.2014.00014. URL https://www.frontiersin.org/article/10.3389/fninf.2014.00014.

[27] Rahul S Desikan, Florent Ségonne, Bruce Fischl, Brian T Quinn, Bradford C Dickerson, Deborah Blacker, Randy L Buckner, Anders M Dale, R Paul Maguire, Bradley T Hyman, et al. An automated labeling system for subdividing the human cerebral cortex on mri scans into gyral based regions of interest. *Neuroimage*, 31(3):968–980, 2006.

[28] Nathalie Tzourio-Mazoyer, Brigitte Landeau, Dimitri Papathanassiou, Fabrice Crivello, Olivier Etard, Nicolas Delcroix, Bernard Mazoyer, and Marc Joliot. Automated anatomical labeling of activations in spm using a macroscopic anatomical parcellation of the mni mri single-subject brain. *Neuroimage*, 15(1):273–289, 2002.

[29] Lindsay M. Alexander, Jasmine Escalera, Lei Ai, Charissa Andreotti, Karina Febre, Alexander Mangone, Natan Vega-Potler, Nicolas Langer, Alexis Alexander, Meagan Kovacs, Shannon Litke, Bridget O'Hagan, Jennifer Andersen, Batya Bronstein, Anastasia Bui, Marijayne Bushey, Henry Butler, Victoria Castagna, Nicolas Camacho, Elisha Chan, Danielle Citera, Jon Clucas, Samantha Cohen, Sarah Dufek, Megan Eaves, Brian Fradera, Judith Gardner, Natalie Grant-Villegas, Gabriella Green, Camille Gregory, Emily Hart, Shana Harris, Megan Horton, Danielle Kahn, Katherine Kabotyanski, Bernard Karmel, Simon P. Kelly, Kayla Kleinman, Bonhwang Koo, Eliza Kramer, Elizabeth Lennon, Catherine Lord, Ginny Mantello, Amy Margolis, Kathleen R. Merikangas, Judith Milham, Giuseppe Minniti, Rebecca Neuhaus, Alexandra Levine, Yael Osman, Lucas C. Parra, Ken R. Pugh, Amy Racanello, Anita Restrepo, Tian Saltzman, Batya Septimus, Russell Tobe, Rachel Waltz, Anna Williams, Anna Yeo, Francisco X. Castellanos, Arno Klein, Tomas Paus, Bennett L. Leventhal, R. Cameron Craddock, Harold S. Koplewicz, and Michael P. Milham. An open resource for transdiagnostic research in pediatric mental health and learning disorders. 4:170181. ISSN 2052-4463. doi: 10.1038/sdata.2017.181. URL https://www.nature.com/articles/sdata2017181.

[30] Korbinian Brodmann. *Vergleichende Lokalisationslehre der GroÃ§hirnrinde : in ihren Prinzipien dargestellt auf Grund des Zellenbaues*. 1909.

[31] Rahul S. Desikan, Florent SÃľgonne, Bruce Fischl, Brian T. Quinn, Bradford C. Dickerson, Deborah Blacker, Randy L. Buckner, Anders M. Dale, R. Paul Maguire, Bradley T. Hyman, Marilyn S. Albert, and Ronald J. Killiany. An automated labeling system for subdividing the human cerebral cortex on MRI scans into gyral based regions of interest. *NeuroImage*, 31(3):968–980, July 2006. ISSN 10538119. doi: 10.1016/j.neuroimage.2006.01.021. URL https://linkinghub.elsevier.com/retrieve/pii/S1053811906000437.

[32] Steven Giavasis, Daniel Clark, Caroline Froehlich, John Pellman, Sharad Sikka, Zarrar Shehzad, Ranjit Khanuja, Brian Cheung, Sebastian Urchs, Qingyang Li, Yaroslav Halchenko, Daniel Lurie, Rosalia Tungaraza, Joshua Vogelstein, Asier Erramuzpe, Aimi Watanabe, Adam Liska, Daniel A

Kessler, Chris Filo Gorgolewski, and R. Cameron Craddock. Fcp-indi/c-pac: Cpac version 1.0.0 beta, 2016. URL https://zenodo.org/record/164638.

[33] Matthew F. Glasser, Timothy S. Coalson, Emma C. Robinson, Carl D. Hacker, John Harwell, Essa Yacoub, Kamil Ugurbil, Jesper Andersson, Christian F. Beckmann, Mark Jenkinson, Stephen M. Smith, and David C. Van Essen. A multi-modal parcellation of human cerebral cortex. *Nature*, 536 (7615):171–178, 2016. ISSN 1476-4687. doi: 10.1038/nature18933.

[34] Jill M. Goldstein, Larry J. Seidman, Nikos Makris, Todd Ahern, Liam M. O'Brien, Verne S. Caviness, David N. Kennedy, Stephen V. Faraone, and Ming T. Tsuang. Hypothalamic abnormalities in schizophrenia: sex effects and genetic vulnerability. *Biological Psychiatry*, 61(8):935–945, April 2007. ISSN 0006-3223. doi: 10.1016/j.biopsych.2006.06.027.

[35] Alexander Schaefer, Ru Kong, Evan M. Gordon, Timothy O. Laumann, Xi-Nian Zuo, Avram J. Holmes, Simon B. Eickhoff, and B. T. Thomas Yeo. Local-Global Parcellation of the Human Cerebral Cortex from Intrinsic Functional Connectivity MRI. *Cerebral Cortex (New York, N.Y.: 1991)*, 28(9):3095–3114, September 2018. ISSN 1460-2199. doi: 10.1093/cercor/bhx179.

[36] J. Talairach and G. Szikla. Application of stereotactic concepts to the surgery of epilepsy. *Acta Neurochirurgica. Supplementum*, 30:35–54, 1980.

[37] N. Tzourio-Mazoyer, B. Landeau, D. Papathanassiou, F. Crivello, O. Etard, N. Delcroix, B. Mazoyer, and M. Joliot. Automated anatomical labeling of activations in SPM using a macroscopic anatomical parcellation of the MNI MRI single-subject brain. *NeuroImage*, 15(1):273–289, January 2002. ISSN 1053-8119. doi: 10.1006/nimg.2001.0978.

[38] Setsu Wakana, Hangyi Jiang, Lidia M. Nagae-Poetscher, Peter C. M. van Zijl, and Susumu Mori. Fiber tract-based atlas of human white matter anatomy. *Radiology*, 230(1):77–87, January 2004. ISSN 0033-8419. doi: 10.1148/radiol.2301021640.

[39] Liang Wang, Ryan E. B. Mruczek, Michael J. Arcaro, and Sabine Kastner. Probabilistic Maps of Visual Topography in Human Cortex. *Cerebral Cortex (New York, N.Y.: 1991)*, 25(10):3911–3931, October 2015. ISSN 1460-2199. doi: 10.1093/cercor/bhu277.

[40] B. T. Thomas Yeo, Fenna M. Krienen, Jorge Sepulcre, Mert R. Sabuncu, Danial Lashkari, Marisa Hollinshead, Joshua L. Roffman, Jordan W. Smoller, Lilla ZÃűllei, Jonathan R. Polimeni, Bruce Fischl, Hesheng Liu, and Randy L. Buckner. The organization of the human cerebral cortex estimated by intrinsic functional connectivity. *Journal of Neurophysiology*, 106(3):1125–1165, September 2011. ISSN 1522-1598. doi: 10.1152/jn.00338.2011.

[41] Lee R Dice. Measures of the amount of ecologic association between species. *Ecology*, 26(3): 297–302, 1945.

[42] K. H. Zou, W. M. Wells, R. Kikinis, and S. K. Warfield. Three validation metrics for automated probabilistic image segmentation of brain tumours. *Stat Med*, 23(8):1259–1282, Apr 2004.

[43] Dekang Lin. *An Information-Theoretic Definition of Similarity*. ICML '98. Kaufmann, San Francisco, Calif, 1998. ISBN 978-1-55860-556-5. URL http://dl.acm.org/citation.cfm?id=645527.657297. OCLC: 246383629.

[44] H. B. Mitchell. Image Similarity Measures. In *Image Fusion*, pages 167–185. Springer Berlin Heidelberg, Berlin, Heidelberg, 2010. ISBN 978-3-642-11215-7 978-3-642-11216-4. doi: 10.1007/978-3-642-11216-4_14. URL http://link.springer.com/10.1007/978-3-642-11216-4_14.

[45] Kunihiko Tateoka. Assessment of Similarity Measures for Accurate Deformable Image Registration. *Journal of Nuclear Medicine & Radiation Therapy*, 03(04), 2012. ISSN 21559619. doi: 10.4172/2155-9619.1000137. URL https://www.omicsonline.org/assessment-of-similarity-measures-for-accurate-deformable-image-registration-2155-9619.1000137.php?aid=18683.

[46] Nguyen Xuan Vinh, Julien Epps, and James Bailey. Information theoretic measures for clusterings comparison: Variants, properties, normalization and correction for chance. 11:2837–2853.

[47] M. J. McAuliffe, F. M. Lalonde, D. McGarry, W. Gandler, K. Csaky, and B. L. Trus. Medical image processing, analysis and visualization in clinical research. In *Proceedings 14th IEEE Symposium*

on Computer-Based Medical Systems. CBMS 2001, pages 381–386, July 2001. doi: 10.1109/CBMS.2001.941749.

[48] Paul McCarthy. Fsleyes, 2019. URL https://zenodo.org/record/1470761.

[49] Wilkin Chau and Anthony R. McIntosh. The talairach coordinate of a point in the MNI space: how to interpret it. 25(2):408–416. ISSN 1053-8119. doi: 10.1016/j.neuroimage.2004.12.007.

[50] Joshua T Vogelstein, Eric W Bridgeford, Qing Wang, Carey E Priebe, Mauro Maggioni, and Cencheng Shen. Discovering and deciphering relationships across disparate data modalities. 8:e41690. ISSN 2050-084X. doi: 10.7554/eLife.41690. URL https://doi.org/10.7554/eLife.41690.

[51] Sambit Panda, Satish Palaniappan, Junhao Xiong, Ananya Swaminathan, Sandhya Ramachandran, Eric W. Bridgeford, Cencheng Shen, and Joshua T. Vogelstein. mgcpy: A comprehensive high dimensional independence testing python package. URL http://arxiv.org/abs/1907.02088.

[52] Gregory Kiar, Eric W. Bridgeford, William R. Gray Roncal, Consortium for Reliability Reproducibility (CoRR), , Vikram Chandrashekhar, Disa Mhembere, Sephira Ryman, Xi-Nian Zuo, Daniel S. Margulies, R. Cameron Craddock, Carey E. Priebe, Rex Jung, Vince D. Calhoun, Brian Caffo, Randal Burns, Michael P. Milham, and Joshua T. Vogelstein. A high-throughput pipeline identifies robust connectomes but troublesome variability. page 188706. doi: 10.1101/188706. URL https://www.biorxiv.org/content/10.1101/188706v4.